Statistica Sinica

LOCALLY SPARSE ESTIMATOR OF GENERALIZED VARYING COEFFICIENT MODEL FOR ASYNCHRONOUS LONGITUDINAL DATA

Rou Zhong[1,2], Chunming Zhang[3], Jingxiao Zhang[1,2,*]

[1]*Center for Applied Statistics, Renmin University of China*

[2]*School of Statistics, Renmin University of China*

[3]*Department of Statistics, University of Wisconsin-Madison*

Abstract: In longitudinal study, it is common that response and covariate are not measured at the same time, which complicates the analysis to a large extent. In this paper, we take into account the estimation of generalized varying coefficient model with such asynchronous observations. A penalized kernel-weighted estimating equation is constructed through kernel technique in the framework of functional data analysis. Moreover, local sparsity is also considered in the estimating equation to improve the interpretability of the estimate. We extend the iteratively reweighted least squares (IRLS) algorithm in our computation. The theoretical properties, including consistency, sparsistency and asymptotic distribution, of the proposed method are established. Simulation studies are conducted to verify the satisfying performance of our method. The method is also applied to a study on women's health to further reveal its practical merits.

---

1. Introduction

Generalized varying coefficient model (Hastie and Tibshirani, 1993; Cai et al., 2000) allows the coefficients to vary over time, which broadens the application of regression models to a large extent. Specifically, the model can be expressed as

$$E\{Y(t)|X(t)\} = g\{\beta_0(t) + \beta_1(t)X(t)\}, t \in \mathcal{T}, \tag{1.1}$$

where $Y(t)$ is the response, $X(t)$ is the covariate, $g(\cdot)$ is a known, strictly increasing and continuously twice-differentiable link function, $\beta_0(t)$ is the intercept function, $\beta_1(t)$ is the varying coefficient function and $\mathcal{T}$ is a bounded and closed interval. In this paper, we tend to develop a new estimating method for generalized varying coefficient model with longitudinal measurements from the perspective of functional data.

In practice, it often happens that covariate and response are not measured at the same time within each subject for longitudinal observations. Such asynchronous observations make the analysis more complicated and there are mainly two types of approaches to solve such issue in the existing work. The first type is two-step and based on synchronizing measurements

of covariate and response. For example, Xiong and Dubin (2010) proposed a binning method to align the measurement times so that traditional longitudinal modeling can be used. Moreover, functional principal component analysis (FPCA) is employed in (Şentürk et al., 2013) to synchronize the data. This type of methods is not ideal enough, since the actual data used for modeling is obtained from estimation and errors from each step will accumulate. The second type is implemented through imposing kernel weight according to the observation time difference between covariate and response. This kind of methods is more appealing, since it makes full use of the whole data. Cao et al. (2015) constructed a kernel weighted estimating equation for generalized linear model and generalized varying coefficient model. Cao et al. (2016) developed a weighted last observation carried forward (LOCF) method. Furthermore, Chen and Cao (2017) applied the kernel weighting technique to partially linear models. Li et al. (2020) considered models with longitudinal functional covariate. Sun et al. (2021) investigated the cases where the observation times are informative. Most of the above kernel methods only adapt to model with time invariant coefficients, and only Cao et al. (2015) thought about the approach of generalized varying coefficient model. However, the varying coefficients are estimated point by point, which can be time-consuming and lacks integrity. Therefore, a new

estimating method is quite essential.

Interpretation of the varying coefficient function $\beta_1(t)$ is a vital part in regression analysis. Moreover, interpretability can be improved through introducing local sparsity, which means the curve can be strictly equal to zero in some subintervals. In the existing work, local sparsity can be achieved by imposing sparseness penalty and was studied for different models. For example, James et al. (2009), Zhou et al. (2013) and Lin et al. (2017) developed locally sparse estimator for scalar-on-function regression model. Tu et al. (2020) employed a group bridge approach to obtain locally sparse estimates for varying coefficient model. Fang et al. (2020) generalized the method in (Lin et al., 2017) to the cases where the response is multivariate. Function-on-function regression model and function-on-scalar regression model were also taken into account by Centofanti et al. (2020) and Wang et al. (2020) respectively. However, to the best of our knowledge, local sparsity has not been considered for generalized varying coefficient model.

In this paper, approaches in functional data analysis (FDA) are utilized, since longitudinal data can be seen as functional data in sparse design and FDA is more effective than pointwise methods. The goal is to propose a novel method that can be applied to the asynchronous data and

can produce more interpretable estimates. Specifically, we construct a new kernel-weighted estimating equation with the consideration of penalty on both roughness and sparseness. To solve the estimating equation, we extend the iteratively reweighted least squares (IRLS) method to our issue and design an innovative algorithm for the computation. The selection of tuning parameters is also considered. We generalize the extended Bayesian information criterion (EBIC) in (Chen and Chen, 2008, 2012), to make it adapt to the asynchronous data so that the roughness parameter and sparseness parameter can be chosen accordingly. Moreover, the number of basis functions is selected through cross-validation (CV). The proposed method for generalized varying coefficient model is called LocKer, as we can get locally sparse estimator of $\beta_1(t)$ from it and the kernel technique is used in the procedure. Furthermore, theoretical properties are also explored in this paper.

The contributions of our work are three-fold. First, we study generalized varying coefficient model in the framework of FDA with the consideration of both asynchronous issue and local sparsity. The problem is of high practical relevance, since it can facilitate the improvement of accuracy, utility and interpretability. Second, the newly presented algorithm can be implemented through the R package `LocKer` that we developed, and the package

is already available on `https://CRAN.R-project.org/package=LocKer`.
Third, we also explore the consistency, sparsistency and asymptotic distribution of our method.

The paper is set out as follows. In Section 2, we illustrate the construction of the penalized kernel-weighted estimating equation and develop a computation algorithm for the proposed LocKer method. Theoretical properties are discussed in Section 3. Simulation studies are conducted in Section 4, in which we explore both accuracy and zero-valued subintervals identifying ability of the method. We apply our method to a study on women's health in Section 5. In Section 6, we conclude this paper with discussion and list some possible extensions.

2. Methodology

2.1 Estimating equation

Suppose that there are n independent subjects in the study. For the i-th subject, let $Y_i(t)$ and $X_i(t)$ be the realization of response process $Y(t)$ and covariate process $X(t)$, respectively. However, only longitudinal measurements are obtained. In specific, for $i = 1, \ldots, n$, we observe

$$Y_i(T_{ij}), j = 1, \ldots, L_i, \quad X_i(S_{ik}), k = 1, \ldots, M_i,$$

where T_{ij} is the j-th observation time of the response, S_{ik} is the k-th observation time of the covariate, L_i is the observation size of the response and M_i is the observation size of the covariate. Refer to Cao et al. (2015), the observation times can be seen as generating from a bivariate counting process

$$N_i(t,s) = \sum_{j=1}^{L_i} \sum_{k=1}^{M_i} I(T_{ij} \leq t, S_{ik} \leq s),$$

where $I(\cdot)$ is the indicator function.

To estimate $\beta_0(t)$ and $\beta_1(t)$ in (1.1), we employ the following basis approximation

$$\beta_0(t) \approx \sum_{l=1}^{L} B_l(t)\gamma_l^{(0)} = \mathbf{B}(t)^\top \boldsymbol{\gamma}^{(0)}, \quad \beta_1(t) \approx \sum_{l=1}^{L} B_l(t)\gamma_l^{(1)} = \mathbf{B}(t)^\top \boldsymbol{\gamma}^{(1)},$$

where $\{B_l(t), l = 1, \ldots, L\}$ are the B-spline basis functions with degree d and M interior knots, $\gamma_l^{(0)}$ and $\gamma_l^{(1)}$ are the corresponding coefficients of $\beta_0(t)$ and $\beta_1(t)$, $\mathbf{B}(t) = (B_1(t), \ldots, B_L(t))^\top$, $\boldsymbol{\gamma}^{(0)} = (\gamma_1^{(0)}, \ldots, \gamma_L^{(0)})^\top$, $\boldsymbol{\gamma}^{(1)} = (\gamma_1^{(1)}, \ldots, \gamma_L^{(1)})^\top$, and $L = M + d + 1$ is the number of basis functions. Here B-spline basis functions are applied, and Zhong et al. (2021) explained the reasons for the wide use of B-spline basis in local sparse estimation. Let $\boldsymbol{\gamma} = (\boldsymbol{\gamma}^{(0)\top}, \boldsymbol{\gamma}^{(1)\top})^\top$, $\widetilde{X}_l(t) = X(t)B_l(t)$ and $\widetilde{\mathbf{X}}(t) = (\widetilde{X}_1(t), \ldots, \widetilde{X}_L(t))^\top$. Then the generalized varying coefficient model (1.1) can be approximated

by

$$E\{Y(t)|X(t)\} = g\Big\{\sum_{l=1}^{L} B_l(t)\gamma_l^{(0)} + \sum_{l=1}^{L} \widetilde{X}_l(t)\gamma_l^{(1)}\Big\} = g\Big\{\widetilde{\mathbf{X}}^{\star}(t)^{\top}\boldsymbol{\gamma}\Big\},$$

where $\widetilde{\mathbf{X}}^{\star}(t) = (\mathbf{B}(t)^{\top}, \widetilde{\mathbf{X}}(t)^{\top})^{\top}$. As did in many papers, such as Lin et al. (2017) and Li et al. (2020), equal sign is used above to denote the approximation. We can get the estimates of $\beta_0(t)$ and $\beta_1(t)$ through the estimation of $\boldsymbol{\gamma}$. To this end, we construct the following penalized kernel-weighed estimating equation

$$U_n(\boldsymbol{\gamma}) = \frac{1}{N_0}\sum_{i=1}^{n}\sum_{j=1}^{L_i}\sum_{k=1}^{M_i} K_h(T_{ij} - S_{ik})\widetilde{\mathbf{X}}_i^{\star}(S_{ik})\Big[Y_i(T_{ij}) - g\big\{\widetilde{\mathbf{X}}_i^{\star}(S_{ik})^{\top}\boldsymbol{\gamma}\big\}\Big]$$

$$- \mathbf{V}_{\rho_0,\rho_1}\boldsymbol{\gamma} - \frac{\partial\mathrm{PEN}_{\lambda}(\boldsymbol{\gamma})}{\partial\boldsymbol{\gamma}} = \mathbf{0}, \tag{2.2}$$

where $N_0 = \sum_{i=1}^{n} L_i M_i$, $\mathbf{V}_{\rho_0,\rho_1} = \mathrm{diag}(\rho_0\mathbf{V}, \rho_1\mathbf{V})$, $\mathbf{V} = \int_{\mathcal{T}} \mathbf{B}^{(2)}(t)\mathbf{B}(t)^{(2)\top}dt$, $\mathbf{B}^{(2)}(t)$ is the second derivative of $\mathbf{B}(t)$, ρ_0 and ρ_1 are the roughness parameters for $\beta_0(t)$ and $\beta_1(t)$, $K_h(t) = K(t/h)/h$, $K(t)$ is a symmetric kernel function, h is the bandwidth, $\mathrm{PEN}_{\lambda}(\boldsymbol{\gamma})$ is the sparseness penalty for $\beta_1(t)$, λ is the sparseness parameter and $\mathbf{0}$ is a zero-valued vector with length $2L$. Here we use $h = \max(\tau_{0.95}, 0.01)$ as the bandwidth, where $\tau_{0.95}$ is the 0.95-quantile of $\min_{j,k}|T_{ij} - S_{ik}|$. For the first term in (2.2), define the kernel-weighted log-likelihood function as

$$\sum_{i=1}^{n}\sum_{j=1}^{L_i}\sum_{k=1}^{M_i}\left\{\frac{Y_i(T_{ij})\theta_{ik} - b(\theta_{ik})}{a(\phi)} + c(Y_i(T_{ij}), \phi)\right\}K_h(T_{ij} - S_{ik}),$$

where $\theta_{ik} = \widetilde{\mathbf{X}}_i^{\star}(S_{ik})^{\top}\boldsymbol{\gamma}$, $b'(\cdot) = g(\cdot)$, $a(\phi)$ and $c(Y_i(T_{ij}), \phi)$ are both constants. Then the first term can be seen as the derivative of the kernel-weighted log-likelihood function by neglecting a constant multiplier. Here we consider all possible pairs of response and covariate measurements, with the kernel weights to control the effect of various pairs, such that measurements with close observation times can be emphasized. The second term is the derivative of the roughness penalty, which is defined as

$$\frac{\rho_0}{2}\int_{\mathcal{T}}\{\beta_0^{(2)}(t)\}^2 dt + \frac{\rho_1}{2}\int_{\mathcal{T}}\{\beta_1^{(2)}(t)\}^2 dt$$
$$=\frac{\rho_0}{2}\boldsymbol{\gamma}^{(0)\top}\mathbf{V}\boldsymbol{\gamma}^{(0)} + \frac{\rho_1}{2}\boldsymbol{\gamma}^{(1)\top}\mathbf{V}\boldsymbol{\gamma}^{(1)} = \frac{1}{2}\boldsymbol{\gamma}^{\top}\mathbf{V}_{\rho_0,\rho_1}\boldsymbol{\gamma},$$

where $\beta_0^{(2)}(t)$ and $\beta_1^{(2)}(t)$ are the second derivatives of $\beta_0(t)$ and $\beta_1(t)$. The third term is the derivative of the sparseness penalty $\text{PEN}_{\lambda}(\boldsymbol{\gamma})$, the expression of which is provided in Section 2.2. Note that the roughness penalty and sparseness penalty are imposed on the estimating equation by their derivatives. Through the computation of (2.2), locally sparse estimator for model (1.1) with asynchronous observations can be obtained. Though we consider generalized varying coefficient model with one covariate here, it can be easily extended to the cases with more covariates.

2.2   Sparseness penalty

In this section, we introduce the sparseness penalty that is utilized in (2.2). We generalized the functional SCAD penalty in (Lin et al., 2017) to achieve local sparsity of $\beta_1(t)$. To be specific, sparseness penalty imposed on $\beta_1(t)$ is defined as

$$\mathcal{L}(\beta_1) = \frac{M+1}{2T} \int_{\mathcal{T}} p_\lambda(|\beta_1(t)|)dt \approx \frac{1}{2} \sum_{m=1}^{M+1} p_\lambda \left(\sqrt{\frac{M+1}{T} \int_{\tau_{m-1}}^{\tau_m} \beta_1^2(t)dt} \right),$$

(2.3)

where T is the length of $\mathcal{T}$, τ_m is the knot of the used B-spline basis, and $p_\lambda(\cdot)$ is the SCAD function suggested in (Fan and Li, 2001). We then transform (2.3) to the penalty of $\boldsymbol{\gamma}$ for the sake of computation. Let $\|\beta_{1[m]}\|_2^2 = \int_{\tau_{m-1}}^{\tau_m} \beta_1^2(t)dt$. By local quadratic approximation $p_\lambda(|v|) \approx p_\lambda(|v_0|) + \frac{1}{2}\{p'_\lambda(|v_0|)/|v_0|\}(v^2 - v_0^2)$ in (Fan and Li, 2001), we have

$$\sum_{m=1}^{M+1} p_\lambda \left(\sqrt{\frac{M+1}{T}} \|\beta_{1[m]}\|_2 \right)$$

$$\approx \sum_{m=1}^{M+1} \left\{ p_\lambda \left(\sqrt{\frac{M+1}{T}} \|\beta_{1[m]}^{(0)}\|_2 \right) + \frac{1}{2} \frac{p'_\lambda \left(\sqrt{\frac{M+1}{T}} \|\beta_{1[m]}^{(0)}\|_2 \right)}{\sqrt{\frac{M+1}{T}} \|\beta_{1[m]}^{(0)}\|_2} \left(\frac{M+1}{T} \|\beta_{1[m]}\|_2^2 - \frac{M+1}{T} \|\beta_{1[m]}^{(0)}\|_2^2 \right) \right\}$$

$$= \frac{1}{2} \sum_{m=1}^{M+1} \sqrt{\frac{M+1}{T}} p'_\lambda \left(\sqrt{\frac{M+1}{T}} \|\beta_{1[m]}^{(0)}\|_2 \right) \frac{\|\beta_{1[m]}\|^2}{\|\beta_{1[m]}^{(0)}\|^2} + C = \sum_{m=1}^{M+1} \boldsymbol{\gamma}^{(0)\top} \mathbf{U}_m \boldsymbol{\gamma}^{(0)} + C$$

$$= \boldsymbol{\gamma}^\top \mathbf{U} \boldsymbol{\gamma} + C,$$

where

$$
\mathbf{U}_m = \sqrt{\frac{M+1}{T}} \frac{p'_\lambda\left(\sqrt{\frac{M+1}{T}}\|\beta^{(0)}_{1[m]}\|_2\right)}{2\|\beta^{(0)}_{1[m]}\|_2} \mathbf{T}_m,
$$

$$
\mathbf{T}_m = \int_{\tau_{m-1}}^{\tau_m} \mathbf{B}(t)\mathbf{B}(t)^\top dt, \quad \mathbf{U} = \mathrm{diag}\left(\mathbf{O}, \sum_{m=1}^{M+1} \mathbf{U}_m\right), \tag{2.4}
$$

$$
C = \sum_{m=1}^{M+1} p_\lambda\left(\sqrt{\frac{M+1}{T}}\|\beta^{(0)}_{1[m]}\|_2\right) - \frac{1}{2}\sum_{m=1}^{M+1}\sqrt{\frac{M+1}{T}} p'_\lambda\left(\sqrt{\frac{M+1}{T}}\|\beta^{(0)}_{1[m]}\|_2\right)\|\beta^{(0)}_{1[m]}\|_2,
$$

and $\mathbf{O}$ is a $L \times L$ matrix with all elements being zero. Here $\|\beta^{(0)}_{1[m]}\|_2$ is

obtained from the initial value or the estimate in the previous iteration.

Then the sparseness penalty in (2.2) can be expressed as

$$
\mathrm{PEN}_\lambda(\boldsymbol{\gamma}) = \frac{1}{2}\boldsymbol{\gamma}^\top\mathbf{U}\boldsymbol{\gamma}.
$$

Here the value of $\mathbf{U}$ depends on the value of $\|\beta^{(0)}_{1[m]}\|_2$, so it will be varied in

the iteration process that is introduced in Section 2.3.

2.3   Algorithm

We generalize the IRLS algorithm to solve our estimating equation proposed

in Section 2.1.   To this end, we first rewrite (2.2) into matrix form and

more notations need to be introduced. Let $\widetilde{\mathbf{X}}^\star_i = (\widetilde{\mathbf{X}}^\star_i(S_{i1}), \ldots, \widetilde{\mathbf{X}}^\star_i(S_{iM_i}))^\top$,

$\widetilde{\mathbf{X}}^\star = (\mathbf{1}^\top_{L_1} \otimes \widetilde{\mathbf{X}}^{\star\top}_1, \ldots, \mathbf{1}^\top_{L_n} \otimes \widetilde{\mathbf{X}}^{\star\top}_n)^\top$, $\mathbf{Y}_i = (Y_i(T_{i1}), \ldots, Y_i(T_{iL_i}))^\top$, $\mathbf{Y} =$

$(\mathbf{Y}^\top_1 \otimes \mathbf{1}^\top_{M_1}, \ldots, \mathbf{Y}^\top_n \otimes \mathbf{1}^\top_{M_n})^\top$, $\boldsymbol{\eta} = \widetilde{\mathbf{X}}^\star\boldsymbol{\gamma}$, $\mathbf{Z} = \boldsymbol{\eta} + \{\mathbf{Y} - g(\boldsymbol{\eta})\}\cdot f'\{g(\boldsymbol{\eta})\}$, $\mathbf{W} =$

$\mathrm{diag}\{K_h(T_{11}-S_{11}), \ldots, K_h(T_{11}-S_{1M_1}), K_h(T_{12}-S_{11}), \ldots, K_h(T_{nL_n}-S_{nM_n})\}$

and $\mathbf{H} = \mathrm{diag}[1/f'\{g(\boldsymbol{\eta})\}]$, where $\otimes$ is the Kronecker product, $\mathbf{1}_{L_i}$ and $\mathbf{1}_{M_i}$ are the vectors of length L_i and M_i with all elements being 1, and $f'(\cdot)$ is the first derivative of $f(\cdot)$ which is the inverse function of $g(\cdot)$. Then the penalized kernel-weighted estimating equation (2.2) becomes

$$U_n(\boldsymbol{\gamma}) = \frac{1}{N_0}\widetilde{\mathbf{X}}^{\star\top}\mathbf{W}\mathbf{H}(\mathbf{Z} - \boldsymbol{\eta}) - \mathbf{V}_{\rho_0,\rho_1}\boldsymbol{\gamma} - \mathbf{U}\boldsymbol{\gamma} = \mathbf{0}, \qquad (2.5)$$

where $\mathbf{H}$, $\mathbf{Z}$, $\boldsymbol{\eta}$ and $\mathbf{U}$ are computed by initial value of $\boldsymbol{\gamma}$ or its estimate in the previous iteration. Through (2.5), the new estimate can be obtained by

$$\widehat{\boldsymbol{\gamma}} = (\widetilde{\mathbf{X}}^{\star\top}\mathbf{W}\mathbf{H}\widetilde{\mathbf{X}}^{\star} + N_0\mathbf{V}_{\rho_1,\rho_2} + N_0\mathbf{U})^{-1}\widetilde{\mathbf{X}}^{\star\top}\mathbf{W}\mathbf{H}\mathbf{Z}. \qquad (2.6)$$

Moreover, referring to (Lin et al., 2017) and (Zhong et al., 2021), the small elements of $\widehat{\boldsymbol{\gamma}}$ are shrunk to zero in the iteration so that $\widetilde{\mathbf{X}}^{\star\top}\mathbf{W}\mathbf{H}\widetilde{\mathbf{X}}^{\star} + N_0\mathbf{V}_{\rho_1,\rho_2} + N_0\mathbf{U}$ would not be singular. Then the estimates of $\beta_0(t)$ and $\beta_1(t)$ are given by

$$\widehat{\beta}_0(t) = \mathbf{B}(t)^\top\widehat{\boldsymbol{\gamma}}^{(0)}, \quad \widehat{\beta}_1(t) = \mathbf{B}(t)^\top\widehat{\boldsymbol{\gamma}}^{(1)}, \qquad (2.7)$$

where $\widehat{\boldsymbol{\gamma}}^{(0)}$ and $\widehat{\boldsymbol{\gamma}}^{(1)}$ are obtained from the final estimate of $\boldsymbol{\gamma}$ via the definition $\boldsymbol{\gamma} = (\boldsymbol{\gamma}^{(0)\top}, \boldsymbol{\gamma}^{(1)\top})^\top$.

Further, the whole algorithm is summarized as follows:

Step 1: Give initial value of $\boldsymbol{\gamma}$. Let $\boldsymbol{\gamma}^{[0]}$ denote the initial value. Here a least squares estimate with kernel weight is used, and the rough-

ness penalty is also considered in the initial estimate, that is $\boldsymbol{\gamma}^{[0]} = (\widetilde{\mathbf{X}}^{\star\top}\mathbf{W}\widetilde{\mathbf{X}}^{\star} + N_0\mathbf{V}_{\rho_1,\rho_2})^{-1}\widetilde{\mathbf{X}}^{\star\top}\mathbf{W}\mathbf{Y}$.

Step 2: Start with $q = 1$, for the q-th iteration,

(1) $\boldsymbol{\eta}^{[q]} = \widetilde{\mathbf{X}}^{\star}\boldsymbol{\gamma}^{[q-1]}$.

(2) $\mathbf{Z}^{[q]} = \boldsymbol{\eta}^{[q]} + \{\mathbf{Y} - g(\boldsymbol{\eta}^{[q]})\} \cdot f'\{g(\boldsymbol{\eta}^{[q]})\}$ and $\mathbf{H}^{[q]} = \text{diag}[1/f'\{g(\boldsymbol{\eta}^{[q]})\}]$.

(3) Compute $\mathbf{U}^{[q]}$ by (2.4).

(4) $\boldsymbol{\gamma}^{[q]} = (\widetilde{\mathbf{X}}^{\star\top}\mathbf{W}\mathbf{H}^{[q]}\widetilde{\mathbf{X}}^{\star} + N_0\mathbf{V}_{\rho_1,\rho_2} + N_0\mathbf{U}^{[q]})^{-1}\widetilde{\mathbf{X}}^{\star\top}\mathbf{W}\mathbf{H}^{[q]}\mathbf{Z}^{[q]}$ according to (2.6).

(5) Repeat Step 2(1)-(4) until convergence.

Step 3: Let $\widehat{\boldsymbol{\gamma}} = \boldsymbol{\gamma}^{[q]}$, then compute $\widehat{\beta}_0(t)$ and $\widehat{\beta}_1(t)$ by (2.7).

2.4   Selection of tuning parameters

Recall that the bandwidth is chosen by $h = \max(\tau_{0.95}, 0.01)$, where $\tau_{0.95}$ is the 0.95-quantile of $\min_{j,k}|T_{ij} - S_{ik}|$. In this section, we discuss the selection of other tuning parameters involved in the computation, including the roughness parameters, sparseness parameter and the number of B-spline basis, with the bandwidth been determined already. For clarity, let $\rho_0 = \rho_1 \triangleq \widetilde{\rho}$, which means $\beta_0(t)$ and $\beta_1(t)$ share the same roughness parameter.

2.4   Selection of tuning parameters

However, our selecting criterion can be easily extended to the case where

$\rho_0 \neq \rho_1$.

The roughness parameter $\widetilde{\rho}$ and the sparseness parameter λ are jointly

considered. We generalize EBIC in (Chen and Chen, 2008, 2012) to make

it adapt to the asynchronous observations. More specifically, define

$$\text{EBIC}(\widetilde{\rho}, \lambda) = \log(\text{Dev}) + df \cdot \log(n_0)/n_0 + \nu \cdot df \cdot \log(2L)/n_0, \qquad (2.8)$$

where Dev represents deviance of the estimate, df is the degree of freedom,

$n_0 = \#\{K_h(T_{ij} - S_{ik}) \neq 0, i = 1, \ldots, n; j = 1, \ldots L_i; k = 1, \ldots, M_i\}$ and

$0 \leq \nu \leq 1$. We use $\nu = 0.5$ as suggested by Huang et al. (2010). Moreover,

Dev is given by

$$\text{Dev} = -2 \sum_{i=1}^{n} \sum_{j=1}^{L_i} \sum_{k=1}^{M_i} \{Y_i(T_{ij})\widehat{\theta}_{ik} - b(\widehat{\theta}_{ik})\} K_h(T_{ij} - S_{ik}),$$

where $\widehat{\theta}_{ik} = g(\widehat{Y}_i(S_{ik}))$. Then with the neglect of some constant, we have

for Gaussian response,

$$\text{Dev} = \sum_{i=1}^{n} \sum_{j=1}^{L_i} \sum_{k=1}^{M_i} \{Y_i(T_{ij}) - \widehat{Y}_i(S_{ik})\}^2 K_h(T_{ij} - S_{ik}),$$

while for Bernoulli response,

$$\text{Dev} = 2 \sum_{i=1}^{n} \sum_{j=1}^{L_i} \sum_{k=1}^{M_i} \left[Y_i(T_{ij}) \log \frac{Y_i(T_{ij})}{\widehat{Y}_i(S_{ik})} + \{1 - Y_i(T_{ij})\} \log \frac{1 - Y_i(T_{ij})}{1 - \widehat{Y}_i(S_{ik})}\right] K_h(T_{ij} - S_{ik}),$$

and for Poisson response,

$$\text{Dev} = 2 \sum_{i=1}^{n} \sum_{j=1}^{L_i} \sum_{k=1}^{M_i} [\widehat{Y}_i(S_{ik}) - Y_i(T_{ij}) \log\{\widehat{Y}_i(S_{ik})\}] K_h(T_{ij} - S_{ik}).$$

Furthermore, *df* is computed by

$$df = \text{tr}\{\widetilde{\mathbf{X}}_{\mathcal{A}}^{\star}(\widetilde{\mathbf{X}}_{\mathcal{A}}^{\star\top}\mathbf{W}_{\mathcal{A}}\widetilde{\mathbf{X}}_{\mathcal{A}}^{\star} + N_0\mathbf{V}_{\rho_1,\rho_2\mathcal{A}})^{-1}\widetilde{\mathbf{X}}_{\mathcal{A}}^{\star\top}\mathbf{W}_{\mathcal{A}}\},$$

where $\mathcal{A}$ is a set indexing the nonzero elements in $\widehat{\boldsymbol{\gamma}}$. For the third term in (2.8), $2L$ is the length of $\boldsymbol{\gamma}$, and if more covariates are considered, it should be varied accordingly.

We choose the number of B-spline basis functions through CV. For a given L, we first select the best $\widetilde{\rho}$ and λ via EBIC, and then the CV score is calculated by the same computing method as Dev when facing response with various distributions. The effect of L is discussed in our simulation study in Section 4.2.

3. Theoretical results

We study the asymptotic properties of our method in this section. Let $\eta(t,\boldsymbol{\beta}) = \beta_0(t) + X(t)\beta_1(t)$, where $\boldsymbol{\beta}(t) = (\beta_0(t),\beta_1(t))^\top$. Let $\boldsymbol{\beta}_0(t)$ be the true value of $\boldsymbol{\beta}(t)$. Define $\mathbf{X}^\star(t) = (1, X(t))^\top$. Let $\text{var}\{Y(t)|X(t)\} = \sigma\{t,X(t)\}^2$ and $\text{cov}\{Y(s),Y(t)|X(s),X(t)\} = r\{s,t,X(s),X(t)\}$. Moreover, denote $\text{NULL}(f) = \{t \in \mathcal{T} : f(t) = 0\}$ and $\text{SUPP}(f) = \{t \in \mathcal{T} : f(t) \neq 0\}$ for any function $f(t)$. Denote $\rho = \max(\rho_0, \rho_1)$. The needed assumptions are listed as follows:

Assumption 1. There exists some constant $c > 0$ such that $|\beta_0^{(p')}(t_1) - \beta_0^{(p')}(t_2)| \leq c|t_1 - t_2|^\nu$ and $|\beta_1^{(p')}(t_1) - \beta_1^{(p')}(t_2)| \leq c|t_1 - t_2|^\nu, \nu \in [0, 1]$. Let $r = p' + \nu$ and assume that $3/2 < r \leq d$, where d is the degree of the B-spline basis.

Assumption 2. The counting process $N_i(t, s)$ is independent of (Y_i, X_i) and $E\{dN_i(t, s)\} = \lambda(t, s)dtds$, where $\lambda(t, s)$ is a bounded twice-continuous differentiable function for any $t, s \in \mathcal{T}$. Borel measure for $\mathcal{G} = \{\lambda(t, t) > 0, t \in \mathcal{T}\}$ is strictly positive. Moreover, $P\{dN(t_1, t_2) = 1|N(s_1, s_2) - N(s_1-, s_2-) = 1\} = f(t_1, t_2, s_1, s_2)dt_1dt_2$ for $t_1 \neq s_1$ and $t_2 \neq s_2$, where $f(t_1, t_2, s_1, s_2)$ is continuous and $f(t_1\pm, t_2\pm, s_1\pm, s_2\pm)$ exists.

Assumption 3. The tuning parameter $\lambda \to 0$ as $n \to \infty$. Assume that $\sqrt{\int_{\text{SUPP}(\beta_1)} p'_\lambda(|\beta_1(t)|)^2 dt} = O(n^{-1/2}M^{-3/2})$, $\sqrt{\int_{\text{SUPP}(\beta_1)} p''_\lambda(|\beta_1(t)|)^2 dt} = o(M^{-3/2})$.

Assumption 4. For any $\boldsymbol{\beta}$ in a neighborhood of $\boldsymbol{\beta}_0$, we assume that $E[\mathbf{X}^\star(s)g\{\eta(t, \boldsymbol{\beta})\}]$ and $E[\mathbf{X}^\star(s)g'\{\eta(t, \boldsymbol{\beta})\}X^b(t)]$ are twice-continuous differentiable for any $(t, s) \in \mathcal{T}^2$, where $b = 0, 1$. Moreover, we assume that $E[\mathbf{X}^\star(s_1)\mathbf{X}^\star(s_2)^\top g\{\eta(t_1, \boldsymbol{\beta})\}g\{\eta(t_2, \boldsymbol{\beta})\}]$ and $E[\mathbf{X}^\star(s_1)\mathbf{X}^\star(s_2)^\top r\{t_1, t_2, X(t_1), X(t_2)\}]$ are twice-continuous differentiable for any $(t_1, t_2, s_1, s_2) \in \mathcal{T}^4$.

Assumption 5. For any $\boldsymbol{\beta}$ in a neighborhood of $\boldsymbol{\beta}_0$, we assume that

$E[\mathbf{X}_2^\star(s)\mathbf{X}_2^\star(s)^\top g'\{\eta(s, \boldsymbol{\beta})\}^2]$ and $E[\mathbf{X}^\star(s)\sigma\{s, X(s)\}^2]$ are uniformly bounded in s, where $\mathbf{X}_2^\star(s) = (1, X^2(t))^\top$.

Assumption 6. If ψ_0 and ψ_1 satisfy $\psi_0(s) + \psi_1(s)X(s) = 0, \forall s \in \mathcal{G}$ with probability 1, then $\psi_0 = 0$ and $\psi_1 = 0$.

Assumption 7. The kernel function $K(\cdot)$ is a symmetric density function. Assume that $\int z^2 K(z)dz < \infty$ and $\int K(z)^2 dz < \infty$.

Assumption 1 is similar to (C2) in (Lin et al., 2017), and this assumption is used to justify the B-spline approximation. Requirement for the counting process is presented in Assumption 2 and is the same as Condition 1 in (Cao et al., 2015) and Assumption 3 in (Li et al., 2020). Assumption 3 is analogous to (C3) in (Lin et al., 2017), while Assumptions 4-6 are parallel to assumptions in (Li et al., 2020). Furthermore, Assumption 7 is a common assumption for kernel function.

Theorem 1. *Under Assumptions 1 - 7, if $M^{1/2}h^2 \to 0$, $n^{-1/2}M^{3/2}h^{-1/2} \to 0$, $\rho \to 0$ and $M^{-r} \to 0$, we have*

$$\sup_{t \in \mathcal{T}} |\widehat{\beta}_0(t) - \beta_0(t)| = O_p(M^{1/2}h^2 + n^{-1/2}M^{1/2}h^{-1/2} + \rho M^{-1/2} + M^{-r}),$$

$$\sup_{t \in \mathcal{T}} |\widehat{\beta}_1(t) - \beta_1(t)| = O_p(M^{1/2}h^2 + n^{-1/2}M^{1/2}h^{-1/2} + \rho M^{-1/2} + M^{-r}).$$

The above theorem states the consistency of both $\beta_0(t)$ and $\beta_1(t)$, and the convergence rates are also given. To achieve the best conver-

gence rate in Theorem 1, we can set $h = O(n^{-1/5})$, $M = O(n^{\frac{4}{5(1+2r)}})$ and $\rho = O(n^{\frac{-4r+2}{5(1+2r)}})$. Then we have $\sup_{t \in \mathcal{T}} |\widehat{\beta}_0(t) - \beta_0(t)| = O_p(n^{\frac{-4r}{5(1+2r)}})$ and $\sup_{t \in \mathcal{T}} |\widehat{\beta}_1(t) - \beta_1(t)| = O_p(n^{\frac{-4r}{5(1+2r)}})$. Further, we discuss the sparsistency of $\beta_1(t)$ in the following theorem.

Theorem 2. *Suppose that the conditions of Theorem 1 are satisfied, if $nh^5 = O(1)$, $nhM^{-2r} = o(1)$, $\rho = o(n^{-1/2})$ and $\lambda n^{1/2} M^{-1/2} h^{1/2} \to \infty$, then we have $NULL(\widehat{\beta}_1) \to NULL(\beta_1)$ and $SUPP(\widehat{\beta}_1) \to SUPP(\beta_1)$ in probability, as $n \to \infty$.*

According to Theorem 2, the zero-valued subintervals of our estimate $\widehat{\beta}_1(t)$ are consistent with the true zero-valued subintervals. That means we have $\widehat{\beta}_1(t) = 0$ for any $t \in \text{NULL}(\beta_1)$ and $\widehat{\beta}_1(t) \neq 0$ for any $t \in \text{SUPP}(\beta_1)$ in probability. Next, we discuss the asymptotic distribution of $\widehat{\boldsymbol{\gamma}}$. Let $\boldsymbol{\gamma}_0 = (\boldsymbol{\gamma}_0^{(0)\top}, \boldsymbol{\gamma}_0^{(1)\top})^\top$ be the coefficient vector that satisfies $\|\boldsymbol{\gamma}_0^{(0)\top} \mathbf{B} - \beta_0\|_\infty = O(M^{-r})$ and $\|\boldsymbol{\gamma}_0^{(1)\top} \mathbf{B} - \beta_1\|_\infty = O(M^{-r})$ (de Boor, 2001; Zhong et al., 2021).

Theorem 3. *Suppose that the conditions of Theorem 1 are satisfied, if $nh^5M = o(1)$, $nhM^{-2r} = O(1)$, $n^{-1}M^2 = o(1)$ and $\rho = o(n^{-1/2})$, then*

$$\frac{nh(\widehat{\boldsymbol{\gamma}} - \boldsymbol{\gamma}_0)^\top \Omega_n^2 (\widehat{\boldsymbol{\gamma}} - \boldsymbol{\gamma}_0) - tr(\Sigma_0)}{\sqrt{2tr(\Sigma_0^2)}} \xrightarrow{d} N(0, 1),$$

where

$$\Omega_n = n^{-1} \sum_{i=1}^{n} \int \int K_h(t-s)\widetilde{\boldsymbol{X}}_i^{\star}(s)g'\{\eta_i(s,\boldsymbol{\beta}_0)\}\widetilde{\boldsymbol{X}}_i^{\star}(s)^{\top} dN_i(t,s),$$

$$\Sigma_0 = var\left(h^{1/2}\int \int K_h(t-s)\widetilde{\boldsymbol{X}}^{\star}(s)[Y(t) - g\{\eta(s,\boldsymbol{\beta}_0)\}]dN(t,s)\right).$$

The asymptotic distribution of $\widehat{\boldsymbol{\gamma}}$ is further studied by simulated data in the Supplementary Material. Moreover, we also explore the point-wise asymptotic distributions of $\widehat{\beta}_0(t)$ and $\widehat{\beta}_1(t)$ and provide the proofs of all theorems in the Supplementary Material.

4. Simulation studies

4.1 Numerical performance

In this section, we discuss the performance of the proposed method through simulation studies. The simulated datasets are generated from model (1.1), and Gaussian response, Bernoulli response and Poisson response are all in consideration. Moreover, for each distribution, both nonsparse coefficient function and coefficient function with local sparsity are taken into account. The detailed settings are as follows:

- Gaussian cases: The intercept function is set as $\beta_0(t) = \cos(2\pi t), t \in [0,1]$. For the nonsparse setting, the coefficient function $\beta_1(t) = \sin(2\pi t)$, while for the sparse setting, $\beta_1(t) = 2 \cdot \{B_6(t) + B_7(t)\}$, where

$B_l(t)$ is the l-th B-spline basis on $[0, 1]$ with degree three and nine e-qually spaced interior knots. We generate the covariate functions in the same way as Lin et al. (2017), that is $X_i(t) = \sum_{l=1} a_{il} B_l^X(t)$, where a_{ij} is obtained from the standard normal distribution and $B_l^X(t)$ is the l-th B-spline basis on $[0, 1]$ with degree four and 69 equally s-paced interior knots. The sample size is set as $n = 200$. Then $Y_i(t)$ is generated from Gaussian distribution with mean $\beta_0(t) + \beta_1(t) X_i(t)$ and standard error one. To get asynchronous data, the observation sizes of response and covariate are generated independently from Poisson distribution with one additional observation to avoid the cases with no measurement. Here response and covariate share the same inten-sity rate m, and m is set to be 15 and 20. Then the observation times are uniformly selected on $[0, 1]$.

- Bernoulli cases: The settings are the same as Gaussian cases, except that $Y_i(t)$ is generated from Bernoulli distribution with mean $\beta_0(t) + \beta_1(t) X_i(t)$.

- Poisson cases: The settings are the same as Gaussian cases, except that $Y_i(t)$ is generated from Poisson distribution with mean $\beta_0(t) + \beta_1(t) X_i(t)$.

The proposed LocKer method is compared with other four approaches in the simulation. The first one is a reconstruction method, that is synchronizing the response and covariate by PACE (Yao et al., 2005) like Şentürk et al. (2013), and then employing the traditional IRLS algorithm. The moment method in (Şentürk et al., 2013), the approach in Cao et al. (2015) and the penalized least squares estimating (PLSE) method investigated by Tu et al. (2020) are also considered. However, Tu et al. (2020) investigated local sparse estimator for varying coefficient model with synchronous observation. So to implement their method for asynchronous cases, we first synchronize the data by smoothing and then apply PLSE to the synchronized data. These four methods are denoted as Recon, Moment, Cao, PLSE respectively for simplicity. Though Cao method is available for regression model with Bernoulli and Poisson response, it is quite slow for these non-Gaussian cases since it is a pointwise method. Hence, identity link is used for Cao method in all considered cases. Moreover, PLSE is only applicable to regression model with Gaussian response, so the responses are seen as to be Gaussian distributed for PLSE in all cases.

4.1   Numerical performance

We evaluate the integrated square error (ISE) of the estimated intercept function and coefficient function for each method. To be specific,

$$\text{ISE}_0 = \int_{\mathcal{T}} \{\widehat{\beta}_0(t) - \beta_0(t)\}^2 dt,$$
$$\text{ISE}_1 = \int_{\mathcal{T}} \{\widehat{\beta}_1(t) - \beta_1(t)\}^2 dt.$$

In the simulation, 100 runs are conducted for each cases. The average ISE and the standard deviation are compared among various methods.

Table 1 reports the averaged ISE_0 and ISE_1 of Gaussian cases. With various settings for coefficient function $\beta_1(t)$ and observation rate m, the simulation results show similar trend. For the estimation of intercept function $\beta_0(t)$, all these five methods give promising results with minor difference on ISE_0. On the other hand, it is evident that our LocKer method exhibits significant advantages for the estimation of $\beta_1(t)$, regardless the true $\beta_1(t)$ is sparse or not. These results demonstrate that synchronizing approach and pointwise approach are not adequate enough, which further indicates the importance of using observed data directly and taking sufficient account of smoothness in estimation. Moreover, it can be seen that more precise estimating results are obtained for each method with the increase of observation rate.

Simulation results for Bernoulli cases are presented in Table 2. The ISE_0 and ISE_1 are observed to be higher compared with the errors in Gaussian cases, which implies that Bernoulli response is more difficult to handle. However, the proposed LocKer still outperforms the other four methods in estimating $\beta_1(t)$ for both nonsparse and sparse settings, though Recon and Moment methods are slightly better in estimating $\beta_0(t)$. The reason for the invalid behaviour of Cao and PLSE methods is that they simply treat the Bernoulli response as Gaussian response here. Furthermore, Table 3 displays the simulation results for Poisson cases. We can find that the proposed LocKer achieves the most accurate estimates for both $\beta_0(t)$ and $\beta_1(t)$ in each considered setting.

In summary, our LocKer method yields encouraging estimating results for each cases in comparison with all the other methods. We conjecture the superiority of our method is due to the employment of FDA approach and kernel technique, as well as the consideration of local sparsity.

4.2   The effect of L

We mainly discuss the accuracy of estimation in Section 4.1. In this section, we tend to explore how the number of B-spline basis functions influences the estimation, especially the ability of identifying zero-valued subintervals

Table 1: The averaged ISE_0 and ISE_1 across 100 runs for five methods in Gaussian cases, with standard deviation in parentheses.

		$n = 200, m = 15$		$n = 200, m = 20$	
		ISE_0	ISE_1	ISE_0	ISE_1
Nonsparse	Recon	0.0050 (0.0022)	0.2768 (0.0505)	0.0044 (0.0019)	0.1889 (0.0455)
	Moment	0.0045 (0.0022)	0.4154 (0.1826)	0.0033 (0.0017)	0.4001 (0.0581)
	Cao	0.0072 (0.0031)	0.3000 (0.0326)	0.0059 (0.0028)	0.2841 (0.0344)
	PLSE	0.0244 (0.0106)	0.3994 (0.0839)	0.0145 (0.0066)	0.2966 (0.0998)
	LocKer	0.0170 (0.0081)	0.0385 (0.0255)	0.0094 (0.0062)	0.0217 (0.0148)
Sparse	Recon	0.0049 (0.0025)	0.2329 (0.0713)	0.0045 (0.0023)	0.1578 (0.0516)
	Moment	0.0052 (0.0059)	0.5350 (0.2588)	0.0033 (0.0016)	0.4972 (0.0648)
	Cao	0.0071 (0.0035)	0.3176 (0.0627)	0.0057 (0.0033)	0.3124 (0.0514)
	PLSE	0.0216 (0.0081)	0.3025 (0.0992)	0.0153 (0.0057)	0.2147 (0.0780)
	LocKer	0.0131 (0.0075)	0.0515 (0.0303)	0.0087 (0.0043)	0.0302 (0.0173)

Table 2: The averaged ISE_0 and ISE_1 across 100 runs for five methods in Bernoulli cases, with standard deviation in parentheses.

		$n = 200, m = 15$		$n = 200, m = 20$	
		ISE_0	ISE_1	ISE_0	ISE_1
Nonsparse	Recon	0.0128 (0.0061)	0.3123 (0.0824)	0.0106 (0.0057)	0.2264 (0.0791)
	Moment	0.0171 (0.0085)	0.6108 (0.3848)	0.0131 (0.0064)	0.4744 (0.2760)
	Cao	0.5600 (0.0139)	0.4530 (0.0133)	0.5590 (0.0135)	0.4480 (0.0142)
	PLSE	0.5132 (0.0170)	0.4856 (0.0195)	0.5163 (0.0150)	0.4721 (0.0255)
	LocKer	0.0531 (0.0267)	0.1777 (0.0973)	0.0332 (0.0155)	0.1074 (0.0578)
Sparse	Recon	0.0182 (0.0075)	0.2898 (0.0966)	0.0172 (0.0067)	0.2444 (0.0892)
	Moment	0.0230 (0.0113)	0.6906 (0.3372)	0.0193 (0.0074)	0.5646 (0.1204)
	Cao	0.5751 (0.0150)	0.5259 (0.0148)	0.5753 (0.0113)	0.5239 (0.0140)
	PLSE	0.5272 (0.0175)	0.5490 (0.0301)	0.5311 (0.0119)	0.5381 (0.0331)
	LocKer	0.0426 (0.0235)	0.2600 (0.1094)	0.0291 (0.0147)	0.1773 (0.0805)

Table 3: The averaged ISE_0 and ISE_1 across 100 runs for five methods in Poisson cases, with standard deviation in parentheses.

		$n = 200, m = 15$		$n = 200, m = 20$	
		ISE_0	ISE_1	ISE_0	ISE_1
Nonsparse	Recon	0.0257 (0.0078)	0.2789 (0.0573)	0.0234 (0.0064)	0.1929 (0.0437)
	Moment	0.0285 (0.0083)	0.3335 (0.1157)	0.0253 (0.0067)	0.3597 (0.0489)
	Cao	1.9949 (0.1056)	0.2645 (0.0378)	1.9772 (0.0794)	0.2496 (0.0371)
	PLSE	1.6426 (0.1044)	0.3555 (0.0909)	1.7170 (0.0942)	0.2408 (0.0773)
	LocKer	0.0163 (0.0103)	0.0345 (0.0186)	0.0096 (0.0069)	0.0192 (0.0128)
Sparse	Recon	0.0660 (0.0166)	0.2462 (0.0940)	0.0660 (0.0146)	0.1670 (0.0903)
	Moment	0.0730 (0.0234)	0.4579 (0.0962)	0.0745 (0.0175)	0.4791 (0.0647)
	Cao	1.8242 (0.0954)	0.4116 (0.0511)	1.8220 (0.0752)	0.3991 (0.0496)
	PLSE	1.4866 (0.0916)	0.4303 (0.1172)	1.5611 (0.0819)	0.3346 (0.1184)
	LocKer	0.0268 (0.0128)	0.0912 (0.0604)	0.0185 (0.0097)	0.0465 (0.0225)

of $\beta_1(t)$. Since local sparsity is also taken into account for PLSE method, we also consider the comparison with PLSE in this section. The setups are the same as the settings in Section 4.1, except that the response and covariate are set to be observed at the same times to make the comparison with PLSE more meaningful. To quantify the identifying ability, we compute the values of $\beta_1(t)$ and $\widehat{\beta}_1(t)$ at a sequence of dense grids on $[0, 1]$, and calculate the rates of grids that correctly identified to be zero and falsely estimated to be zero, which are denoted by TP and FN respectively. Moreover, the closer TP is to 1 and the closer FN is to 0, the better the identifying ability is.

Tables 4-5 list the simulation results with the use of different values of L in Gaussian cases. For the nonsparse settings, ISE_0 and ISE_1 of the proposed LocKer method decrease with the increase of L, and they are better than that of PLSE. Moreover, TP does not exist for nonsparse settings, so only FN is reported. Here both methods achieve zero-valued FN, which means no grid is falsely identified, indicating that subintervals can be effectively identified for coefficient function without local sparsity by both methods.

For the sparse settings, while the estimation of $\beta_0(t)$ becomes better with the growth of L, we find that both methods give the best estimation of $\beta_1(t)$ when $L = 13$. The reason is related to the setting of $\beta_1(t)$. Recall

that to ensure local sparsity of $\beta_1(t)$, we utilize the B-spline basis with degree three and nine equally spaced interior knots in the setup. Therefore, B-spline basis used in the setup is coincided with B-spline basis applied in the estimation, which leads to the nice performance of our method for $L = 13$. Except the cases where $L = 13$, it is obvious that larger value of L can make better estimation in terms of both accuracy and identifying ability. Compared with PLSE, our method produces more precise estimate for $\beta_0(t)$, but ISE_1 is slightly higher than that of PLSE. However, as for the identifying ability, the proposed LocKer method is much better than PLSE according to both TP and FN, which shows the advantage of our method in zero-valued subintervals identification.

To sum up, though larger value of L is beneficial for the identification in some general cases, it should be realized that more B-spline basis functions would bring more parameters in the estimation, thus increase the difficulty of estimation. Furthermore, discussion about the results in Bernoulli and Poisson cases is provided in the Supplementary Material.

5. Real data analysis

In the life of women, menopausal transition is a very important issue and many physical changes can be happened during this period. For example,

Table 4: The averaged ISE_0, ISE_1, TP and FN across 100 runs for PLSE and LocKer using various values of L when $n = 200, m = 15$ in Gaussian cases, with standard deviation in parentheses.

		ISE_0	ISE_1	TP	FN
$L = 10$	Nonsparse				
	PLSE	0.0120 (0.0054)	0.0196 (0.0064)	–	0 (0)
	LocKer	0.0115 (0.0039)	0.0139 (0.0048)	–	0 (0)
	Sparse				
	PLSE	0.0209 (0.0079)	0.0159 (0.0062)	0.1740 (0.2254)	0 (0)
	LocKer	0.0099 (0.0036)	0.0169 (0.0060)	0.5564 (0.1486)	0 (0)
$L = 13$	Nonsparse				
	PLSE	0.0123 (0.0049)	0.0189 (0.0060)	–	0 (0)
	LocKer	0.0077 (0.0029)	0.0115 (0.0054)	–	0 (0)
	Sparse				
	PLSE	0.0209 (0.0075)	0.0070 (0.0049)	0.6109 (0.3012)	0 (0)
	LocKer	0.0065 (0.0031)	0.0056 (0.0041)	0.9777 (0.0625)	0 (0)
$L = 15$	Nonsparse				
	PLSE	0.0093 (0.0038)	0.0186 (0.0064)	–	0 (0)
	LocKer	0.0063 (0.0025)	0.0095 (0.0054)	–	0 (0)
	Sparse				
	PLSE	0.0152 (0.0059)	0.0081 (0.0039)	0.3925 (0.2461)	0.0230 (0.0365)
	LocKer	0.0053 (0.0022)	0.0161 (0.0072)	0.8619 (0.0461)	0.0195 (0.0359)
$L = 20$	Nonsparse				
	PLSE	0.0093 (0.0039)	0.0204 (0.0062)	–	0 (0)
	LocKer	0.0047 (0.0021)	0.0076 (0.0055)	–	0 (0)
	Sparse				
	PLSE	0.0179 (0.0065)	0.0098 (0.0049)	0.5022 (0.2323)	0.0786 (0.0619)
	LocKer	0.0043 (0.0018)	0.0135 (0.0092)	0.9086 (0.0631)	0.0042 (0.0167)

Table 5: The averaged ISE_0, ISE_1, TP and FN across 100 runs for PLSE and LocKer using various values of L when $n = 200, m = 20$ in Gaussian cases, with standard deviation in parentheses.

			ISE_0	ISE_1	TP	FN
$L = 10$	Nonsparse	PLSE	0.0065 (0.0031)	0.0128 (0.0049)	–	0 (0)
		LocKer	0.0071 (0.0027)	0.0089 (0.0044)	–	0 (0)
	Sparse	PLSE	0.0128 (0.0057)	0.0136 (0.0051)	0.1621 (0.2108)	0 (0)
		LocKer	0.0061 (0.0027)	0.0159 (0.0045)	0.5587 (0.1517)	0 (0)
$L = 13$	Nonsparse	PLSE	0.0066 (0.0029)	0.0131 (0.0045)	–	0 (0)
		LocKer	0.0045 (0.0020)	0.0075 (0.0046)	–	0 (0)
	Sparse	PLSE	0.0143 (0.0046)	0.0050 (0.0033)	0.6009 (0.2522)	0 (0)
		LocKer	0.0038 (0.0016)	0.0049 (0.0034)	0.9838 (0.0542)	0 (0)
$L = 15$	Nonsparse	PLSE	0.0056 (0.0023)	0.0134 (0.0044)	–	0 (0)
		LocKer	0.0041 (0.0018)	0.0075 (0.0043)	–	0 (0)
	Sparse	PLSE	0.0092 (0.0035)	0.0064 (0.0035)	0.3104 (0.2266)	0.0126 (0.0261)
		LocKer	0.0033 (0.0014)	0.0096 (0.0038)	0.8654 (0.0613)	0.0241 (0.0345)
$L = 20$	Nonsparse	PLSE	0.0065 (0.0024)	0.0150 (0.0047)	–	0 (0)
		LocKer	0.0035 (0.0018)	0.0057 (0.0039)	–	0 (0)
	Sparse	PLSE	0.0128 (0.0049)	0.0078 (0.0033)	0.5393 (0.1997)	0.0748 (0.0582)
		LocKer	0.0028 (0.0015)	0.0073 (0.0033)	0.9484 (0.0242)	0.0116 (0.0268)

follicle stimulating hormone (FSH) begins to increase in the perimenopausal stage (Wang et al., 2020). Some studies showed that FSH has an influence on cardiovascular disease (CVD) risk (El Khoudary et al., 2016; Wang et al., 2017), and Serviente et al. (2019) thought that the association between FSH and CVD risk may be related to the effect of FSH on lipid levels. In this section, we aim to explore the relationship between FSH and triglycerides (TG), one of the lipid variables, by the proposed LocKer method.

The Study of Womens Health Across the Nation (SWAN) focuses on the health of women during their middle years. Between 1996 and 1997, there are 3302 women enrolled in this study and ten visits were conducted from 1997 to 2008. Moreover, both FSH and TG were recorded in this study and the data can be download from `https://www.swanstudy.org/`. Since TG was not measured in the last two visits, only the baseline and the first eight visits are taken into account in our analysis. Further, we exclusively consider women that were early perimenopause and pre-menopausal at baseline. Then, after removing individuals that had no measurements of FSH or TG, there remains $n = 3224$ women in the study. Figure 1 displays the observation times of FSH and TG for 100 randomly selected women, and note that the observation times are transformed to be $[0, 1]$-valued. It is shown that some of the observation times for FSH and TG are the same,
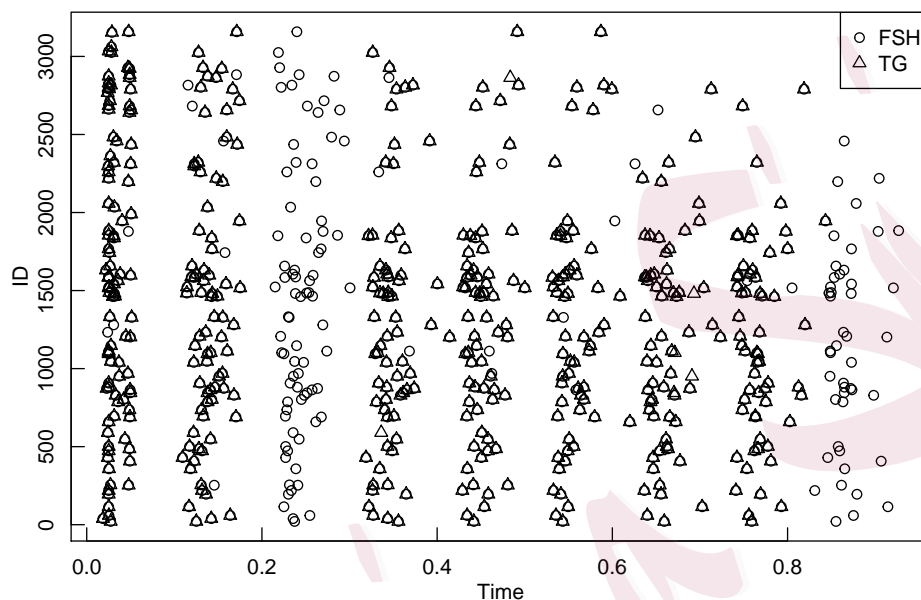
Figure 1: Observation times of FSH and TG for 100 randomly selected women in real data analysis.

but the asynchronous issue still exists. The asynchronous problem is especially serious on $[0.2, 0.3]$ and $[0.8, 1]$ due to the absence of TG records in the second and eighth visits.

The LocKer method is applied by treating FSH as the covariate and treating TG as the response. Both FSH and TG are centralized after being log-transformed. The roughness parameter and sparseness parameter are selected as introduced in Section 2.4. Figure 2 shows the estimated

coefficient function by LocKer. It can be observed that the result reveals negative association between FSH and TG, which is consistent with the discovery of Wang et al. (2020). Furthermore, additional findings can be achieved by local sparsity of our estimate. The estimate is zero-valued in the early stage, which indicates that FSH has minor effect on TG at the start of the menopausal transition. The influence begins to rise at about $t = 0.5$ and reaches the maximum at around $t = 0.8$, which implies greater relationship between FSH and TG in the later stage.

6. Conclusion and discussion

In this paper, we employ FDA method in the estimation of generalized varying coefficient model. Moreover, kernel technique is utilized to solve the asynchronous issue and a sparseness penalty is imposed to improve accuracy and interpretability of the estimates. The theoretical study verifies both consistency and sparsistency of the proposed LocKer method, and also provides asymptotic distribution of the estimator. The extensive simulation experiments and practical application also suggest the encouraging performance of LocKer method.

However, the main focus of this paper is generalized varying coefficient model, which means only the response value and covariate value recorded
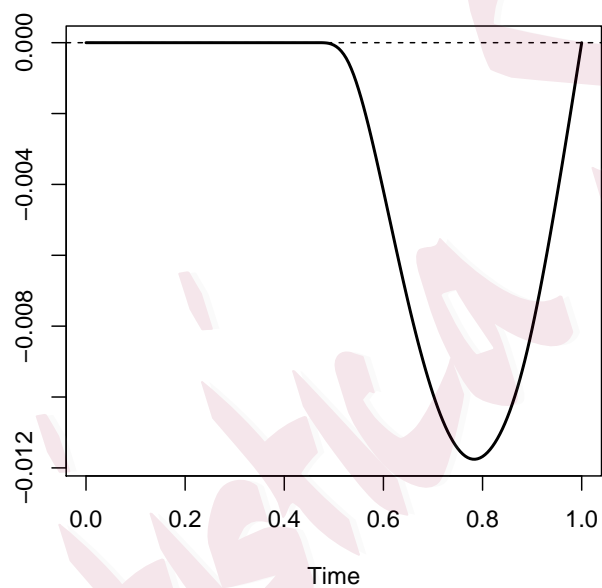
Figure 2: Estimate of the coefficient function obtained by the proposed LocKer method in the exploration of the relationship between FSH and TG for women from the SWAN study.

at the same time are relevant. A more general model can be expressed as

$$E\{Y(t)|X(s), s \in \mathcal{T}\} = g\Big\{\beta_0(t) + \int_{\mathcal{T}} X(s)\beta_1(s,t)ds\Big\}, t \in \mathcal{T}.$$

In the above model, the response is related to the value of covariate on the whole interval $\mathcal{T}$ rather than at one exact time point, which is more practical in the analysis of real world dataset. Furthermore, the consideration of asynchronous issue and local sparsity in this model is also quite essential but in high difficulty, which is the interest of our future research.

Supplementary Materials

The Supplementary Material contains the proofs of Theorems 1-3, and some additional theoretical and simulation results are also provided.

Acknowledgements

References

Cai, Z., J. Fan, and R. Li (2000). Efficient estimation and inferences for varying-coefficient
models. *Journal of the American Statistical Association 95*(451), 888–902.

Cao, H., J. Li, and J. P. Fine (2016). On last observation carried forward and asynchronous
longitudinal regression analysis. *Electronic Journal of Statistics 10*(1), 1155–1180.

Cao, H., D. Zeng, and J. P. Fine (2015). Regression analysis of sparse asynchronous longitudinal
data. *Journal of the Royal Statistical Society: Series B (Statistical Methodology) 77*(4),
755–776.

Centofanti, F., M. Fontana, A. Lepore, and S. Vantini (2020). Smooth lasso estimator for the
function-on-function linear regression model. *arXiv preprint arXiv:2007.00529*.

Chen, J. and Z. Chen (2008). Extended bayesian information criteria for model selection with
large model spaces. *Biometrika 95*(3), 759–771.

Chen, J. and Z. Chen (2012). Extended bic for small-n-large-p sparse glm. *Statistica Sinica*,
555–574.

Chen, L. and H. Cao (2017). Analysis of asynchronous longitudinal data with partially linear
models. *Electronic Journal of Statistics 11*(1), 1549–1569.

de Boor, C. R. (2001). *A practical guide to splines*. New York: Springer-Verlag.

REFERENCES

El Khoudary, S. R., N. Santoro, H.-Y. Chen, P. G. Tepper, M. M. Brooks, R. C. Thurston, I. Janssen, S. D. Harlow, E. Barinas-Mitchell, F. Selzer, et al. (2016). Trajectories of estradiol and follicle-stimulating hormone over the menopause transition and early markers of atherosclerosis after menopause. *European journal of preventive cardiology 23*(7), 694–703.

Fan, J. and R. Li (2001). Variable selection via nonconcave penalized likelihood and its oracle properties. *Journal of the American statistical Association 96*(456), 1348–1360.

Fang, K., X. Zhang, S. Ma, and Q. Zhang (2020). Smooth and locally sparse estimation for multiple-output functional linear regression. *Journal of statistical computation and simulation 90*(2), 341–354.

Hastie, T. and R. Tibshirani (1993). Varying-coefficient models. *Journal of the Royal Statistical Society: Series B (Methodological) 55*(4), 757–779.

Huang, J., J. L. Horowitz, and F. Wei (2010). Variable selection in nonparametric additive models. *Annals of statistics 38*(4), 2282–2313.

James, G. M., J. Wang, and J. Zhu (2009). Functional linear regression thats interpretable. *The Annals of Statistics 37*(5A), 2083–2108.

Li, T., T. Li, Z. Zhu, and H. Zhu (2020). Regression analysis of asynchronous longitudinal functional and scalar data. *Journal of the American Statistical Association*, 1–15.

Lin, Z., J. Cao, L. Wang, and H. Wang (2017). Locally sparse estimator for functional linear regression models. *Journal of Computational and Graphical Statistics 26*(2), 306–318.

REFERENCES

Şentürk, D., L. S. Dalrymple, S. M. Mohammed, G. A. Kaysen, and D. V. Nguyen (2013). Modeling time-varying effects with generalized and unsynchronized longitudinal data. *Statistics in Medicine 32*(17), 2971–2987.

Serviente, C., T.-P. Tuomainen, J. Virtanen, S. Witkowski, L. Niskanen, and E. Bertone-Johnson (2019). Follicle stimulating hormone is associated with lipids in postmenopausal women. *Menopause: The Journal of The North American Menopause Society 26*(5), 540–545.

Sun, D., H. Zhao, and J. Sun (2021). Regression analysis of asynchronous longitudinal data with informative observation processes. *Computational Statistics & Data Analysis 157*, 107161.

Tu, C. Y., J. Park, and H. Wang (2020). Estimation of functional sparsity in nonparametric varying coefficient models for longitudinal data analysis. *Statistica Sinica 30*(1), 439–465.

Wang, N., H. Shao, Y. Chen, F. Xia, C. Chi, Q. Li, B. Han, Y. Teng, and Y. Lu (2017). Follicle-stimulating hormone, its association with cardiometabolic risk factors, and 10-year risk of cardiovascular disease in postmenopausal women. *Journal of the American Heart Association 6*(9), e005918.

Wang, X., H. Zhang, Y. Chen, Y. Du, X. Jin, and Z. Zhang (2020). Follicle stimulating hormone, its association with glucose and lipid metabolism during the menopausal transition. *Journal of Obstetrics and Gynaecology Research 46*(8), 1419–1424.

Wang, Z., J. Magnotti, M. S. Beauchamp, and M. Li (2020). Functional group bridge for simultaneous regression and support estimation. *arXiv preprint arXiv:2006.10163*.

REFERENCES

Xiong, X. and J. A. Dubin (2010). A binning method for analyzing mixed longitudinal data measured at distinct time points. *Statistics in medicine 29*(18), 1919–1931.

Yao, F., H.-G. Müller, and J.-L. Wang (2005). Functional data analysis for sparse longitudinal data. *Journal of the American statistical association 100*(470), 577–590.

Zhong, R., S. Liu, H. Li, and J. Zhang (2021). Sparse logistic functional principal component analysis for binary data. *arXiv preprint arXiv:2109.08009*.

Zhou, J., N.-Y. Wang, and N. Wang (2013). Functional linear model with zero-value coefficient function at sub-regions. *Statistica Sinica 23*(1), 25.

Center for Applied Statistics, School of Statistics, Renmin University of China, P.R.China

E-mail: zhong_rou@163.com

Department of Statistics, University of Wisconsin-Madison, USA

E-mail: cmzhang@stat.wisc.edu

Center for Applied Statistics, School of Statistics, Renmin University of China, P.R.China

E-mail: zhjxiaoruc@163.com